
Article:
Green, A.M. and Goodwin, S.P. (2007) On mini-halo encounters with stars. Monthly Notices of the Royal Astronomical Society, 375 (3). pp. 1111-1120. ISSN 0035-8711

https://doi.org/10.1111/j.1365-2966.2007.11397.x

Mon. Not. R. Astron. Soc. **375,** 1111–1120 (2007) doi:10.1111/j.1365-2966.2007.11397.x

On mini-halo encounters with stars

Anne M. Green[1]★ and Simon P. Goodwin[2]
[1]*School of Physics and Astronomy, University of Nottingham, Nottingham NG7 2RD*
[2]*Department of Physics and Astronomy, University of Sheffield, Sheffield S3 7RH*

Accepted 2006 December 8. Received 2006 December 7; in original form 2006 April 6

ABSTRACT

We study, analytically and numerically, the energy input into dark matter mini-haloes by interactions with stars. We find that the fractional energy input in simulations of Plummer spheres agrees well with the impulse approximation for small and large impact parameters, with a rapid transition between these two regimes. Using the impulse approximation, the fractional energy input at large impact parameters is fairly independent of the mass and density profiles of the mini-halo; however, low-mass mini-haloes experience a greater fractional energy input in close encounters. We formulate a fitting function which encodes these results and use it to estimate the disruption time-scales of mini-haloes, taking into account the stellar velocity dispersion and mass distribution. For mini-haloes with mass $M < \mathcal{O}(10^{-7}\,\mathrm{M}_{\odot})$ on typical orbits which pass through the disc, we find that the estimated disruption time-scales are independent of mini-halo mass, and are of the order of the age of the Milky Way. For more massive mini-haloes, the estimated disruption time-scales increase rapidly with increasing mass.

Key words: Galaxy: structure – dark matter.

1 INTRODUCTION

In cold dark matter (CDM) cosmologies, structure forms hierarchically; small haloes form first, with larger haloes forming via mergers and accretion. The internal structure of haloes is determined by the dynamical processes, for instance, tidal stripping and dynamical friction, which act on the component subhaloes. Numerical simulations find that substantial amounts of substructure survive within larger haloes (Klypin et al. 1999; Moore et al. 1999) with the number density of subhaloes increasing with decreasing mass, down to the resolution limit of the simulations. Natural questions to ask are: what are the properties of the first dark matter (DM) haloes to form in the Universe, and do significant numbers survive to the present day?

Weakly interacting massive particles (WIMPs) are one of the best-motivated DM candidates. They generically have roughly the required present-day density, and supersymmetry (an extension of the standard model of particle physics) provides a well-motivated WIMP candidate, the lightest neutralino (see e.g. Bertone, Hooper & Silk 2005). Numerous experiments are underway attempting to detect WIMPs either directly (via elastic scattering off target nuclei in the laboratory) or indirectly (via the products of their annihilation). In both cases, the expected signals depend critically on the DM distribution on small scales; direct detection probes the DM on submilliparsec (au) scales, while clumping may enhance the indirect signals. Therefore, the fate of the first DM haloes, and the resulting DM distribution on small (subparsec) scales, is important for practical reasons too.

Studies of the microphysics of WIMPs show that kinetic decoupling and free-streaming combine to produce a cut-off in the density perturbation spectrum for generic WIMPs at a comoving wavenumber $k \sim \mathcal{O}(1\,\mathrm{pc}^{-1})$ (Hofmann, Schwarz & Stöcker 2001; Schwarz, Hofmann & Stöcker 2001; Berezinsky, Dokuchaev & Eroshenko. 2003; Green, Hofmann & Schwarz 2004, 2005; Loeb & Zaldarriaga 2005; Berezinsky, Dokuchaev & Eroshenko 2006) which corresponds to a mass of the order of $10^{-6}\,\mathrm{M}_{\odot}$. Analytic calculations, using linear theory and the spherical collapse model, find that the first typical (i.e. forming from 1σ fluctuations) haloes form at $z \sim 60$ and have radius $R \sim \mathcal{O}(0.01\,\mathrm{pc})$ (Green et al. 2004, 2005).

Diemand, Moore & Stadel (2005) carried out numerical simulations using as input the linear power spectrum for a generic WIMP with mass $m_{\chi} = 100\,\mathrm{GeV}$ (Green et al. 2004, 2005). They used a multiscale technique, twice re-simulating at higher resolution an 'average' region selected from a larger simulation. These simulations confirmed the analytic estimates of the mass and formation redshift of the first mini-haloes and also provided further information about their properties, in particular, the density profiles of sample mini-haloes. The simulations were stopped at $z \approx 26$ when the high-resolution region began to merge with the lower-resolution surroundings, and so the subsequent evolution of the mini-haloes has to be studied separately.

Extensive work has been done on the dynamical evolution of more-massive ($M > 10^{6}\,\mathrm{M}_{\odot}$) substructure (e.g. Zenter & Bullock

★E-mail: anne.green@nottingham.ac.uk (AMG); s.goodwin@sheffield.ac.uk (SPG)

2003; Oguri & Lee 2004; Taylor & Babul 2004; Peñarrubia & Benson 2005). The physics of mini-haloes is significantly different from that of these more-massive haloes, however. First, the first generation of mini-haloes form monolithically, rather than hierarchically. Secondly, the amplitude of the density perturbations on these scales is a very weak function of scale, so that haloes with a range of masses form at the same time. Finally, as well as being subject to the same dynamical processes as larger subhaloes (e.g. tidal stripping, interactions between subhaloes[1]) mini-haloes can lose energy, and possibly be completely disrupted, via interactions with compact objects such as stars. Various authors have used the impulse approximation to investigate the disruption of $M \sim 10^{-6}\,\mathrm{M}_\odot$ mini-haloes due to encounters with stars (Diemand et al. 2005; Moore et al. 2005; Zhao et al. 2005, 2007; Angus & Zhao 2006; Berezinsky et al. 2006; Goerdt et al. 2006). The results of these studies range from most of the mini-haloes surviving disruption (Diemand et al. 2005; Moore et al. 2005) to most of the mini-haloes whose orbits pass through the solar neighbourhood being destroyed (Zhao et al. 2005). A definitive study will have to combine accurate calculations of the response of mini-haloes to individual interactions with simulations of mini-halo orbits in a realistic Galactic potential (see Moore 1993; Zhao et al. 2007, for work in this direction).

In this paper, we use *N*-body simulations to investigate the accuracy of the impulse approximation for calculating the energy input into a mini-halo by an interaction with a star. We formulate a fitting function which matches the results of the simulations and use it to estimate the time-scales for one-off and multiple disruption as a function of mini-halo mass. We caution, and discuss in more detail below, that it is actually the mass loss which is key to determining the extent to which a mini-halo is disrupted. The relationship between the energy input and the mass lost in an interaction is a complex, and to some extent unresolved, problem (see e.g. Aguilar & White 1985; Goerdt et al. 2006).

2 PREVIOUS CALCULATIONS

The duration of a typical star–mini-halo encounter is far shorter than the dynamical time-scale of the mini-halo; therefore, the impulse approximation holds and the interaction can be treated as instantaneous (Spitzer 1958). More specifically, the validity of the impulse approximation can be parametrized by the adiabatic parameter (Gnedin & Ostriker 1999) $x = \omega\tau$ where $\omega = \sigma(b)/b$ is the orbital frequency of particles at a distance b from the centre of the mini-halo and $\tau = 2R/v$ is the duration of the encounter. The impulse approximation is valid if $x \ll 1$, or equivalently $R/b \ll v/\sigma(b)$. As the typical relative velocity of encounters [$v \sim \mathcal{O}(10\text{–}100\,\mathrm{km\,s^{-1}})$] is far larger than the mini-halo velocity dispersion [$\sigma(R) \sim \mathcal{O}(1\,\mathrm{m\,s^{-1}})$], then only for very rare, slow interactions at very small impact parameters will the impulse approximation be violated. The change in the velocity of a particle within an extended body of radius R at position $\boldsymbol{r}$ relative to the centre of the body due to an impulsive interaction with a perturber of mass $M_\star$, moving with relative velocity $\boldsymbol{v}$ at an impact parameter $\boldsymbol{b}$, such that $b \gg R$, is given by (Spitzer 1958):

$$\delta\boldsymbol{v} \approx \frac{2GM_\star}{vb^2}\left[2(\boldsymbol{r}\cdot\boldsymbol{e}_b)\boldsymbol{e}_b + (\boldsymbol{r}\cdot\boldsymbol{e}_v)\boldsymbol{e}_v - \boldsymbol{r}\right], \tag{1}$$

where $\boldsymbol{e}_v$ and $\boldsymbol{e}_\mathbf{b}$ are unit vectors perpendicular to $\boldsymbol{v}$ and $\boldsymbol{b}$, respectively. The energy input, per unit mass, for an individual particle is $\delta E = \boldsymbol{v}\cdot(\delta\boldsymbol{v}) + 0.5(\delta\boldsymbol{v})^2$, and the total energy input into the body is then found by integrating over the density distribution. For a spherically symmetric body, the first term averages to zero and, using the approximation that $(\boldsymbol{r}\cdot\boldsymbol{e}_v)^2 = (\boldsymbol{r}\cdot\boldsymbol{e}_b)^2 \approx r^2/3$, the total energy input is given by

$$\Delta E(b) \approx \frac{4\alpha^2}{3}\frac{G^2M_\star^2MR^2}{v^2b^4}, \tag{2}$$

where

$$\alpha^2 = \frac{\langle r^2\rangle}{R^2} \equiv \frac{1}{R^2}\left[\frac{\int_0^R \mathrm{d}^3\boldsymbol{r}\, r^2\rho(r)}{M}\right], \tag{3}$$

is the rms radius.

For small impact parameter interactions, $b/R \to 0$ (e.g. Gerhard & Fall 1983; Carr & Sakellariadou 1999):

$$\delta\boldsymbol{v} \approx \frac{2GM_\star}{v}\left[\frac{(\boldsymbol{r}\cdot\boldsymbol{e}_v)\boldsymbol{e}_v - \boldsymbol{r}}{\boldsymbol{r}^2 - (\boldsymbol{r}\cdot\boldsymbol{e}_v)^2}\right], \tag{4}$$

so that the energy input is given by

$$\Delta E(b=0) \approx 3\beta^2\frac{G^2M_\star^2M}{v^2R^2}, \tag{5}$$

where

$$\beta^2 = \langle r^{-2}\rangle R^2 \equiv R^2\left[\frac{\int_0^R \mathrm{d}^3\boldsymbol{r}\, r^{-2}\rho(r)}{M}\right], \tag{6}$$

is the rms inverse radius. Carr & Sakellariadou (1999) (drawing on Gerhard & Fall 1983) interpolated between the $b \gg R$ and $b \ll R$ regimes using

$$\delta\boldsymbol{v} = \frac{2GM_\star}{v}\frac{1}{b^2 + (2r^2/3)} \times\left[\frac{2b^2}{b^2 + (2r^2/3)}(\boldsymbol{r}\cdot\boldsymbol{e}_b)\boldsymbol{e}_b + (\boldsymbol{r}\cdot\boldsymbol{e}_v)\boldsymbol{e}_v - \boldsymbol{r}\right], \tag{7}$$

so that

$$\Delta E(b) \approx \frac{4}{3}\left(\frac{GM_\star}{vb^2}\right)^2 \times\int_0^R \mathrm{d}^3\boldsymbol{r}\, r^2\rho(r)\left(1 + \frac{4r^4}{9b^4}\right)\left(1 + \frac{2r^2}{3b^2}\right)^{-4}. \tag{8}$$

Moore (1993) simulated encounters between globular clusters, modelled with King profiles, and massive ($\sim 10^4\,\mathrm{M}_\odot$) black holes. He found that the energy input was well fitted by

$$\Delta E(b) = \frac{\Delta E(b=0)}{[1 + (b/R)]^4}. \tag{9}$$

This fitting function will, however, only reproduce the asymptotic limits, equations (2) and (5), if $\alpha^2 \approx 9\beta^2/4$, which need not be (and we will see is not) the case in general. A simple modification to equation (9),

$$\Delta E(b) = \frac{\Delta E(b=0)}{\left[1 + (bA^{-1/4}/R)\right]^4}, \tag{10}$$

with $A = 4\alpha^2/9\beta^2$, produces a function with the correct asymptotic limits in general.

For later convenience, we write the fractional energy input, which is simply $\Delta E(b)$ divided by the total energy of the mini-halo $E = \gamma GM^2/R$, where γ is a constant of the order of 1 which depends on the density profile (and cut-off radius if one is imposed), as

$$\frac{\Delta E(b)}{E} = \left(\frac{\Delta E(b)}{E}\right)_{\mathrm{fid}}\left[\left(\frac{M_\star}{\mathrm{M}_\odot}\right)\left(\frac{300\,\mathrm{km\,s^{-1}}}{v}\right)\right]^2, \tag{11}$$

[1] See Berezinsky et al. (2003) and Berezinsky et al. (2006) for analytic studies of the effects of interactions between mini-haloes.

Table 1. Structure parameters, binding energy per unit mass and mass of the best-fitting profiles for the three sample haloes (using only the data at radii greater than the force softening). For the energy and mass calculations, a sharp cut-off is taken at $R = r_{200}(z = 26) = 0.03$ and 0.008 pc for halo 1 and haloes 2 and 3, respectively. The final column is the Plummer, core or scale radius for the Plummer, CIS or NFW profile, respectively.

Halo	Profile	$\alpha^2 R^2$ (pc^2)	β^2/R^2 (pc^{-2})	E/M (erg $M_\odot^{-1}$)	M ($M_\odot$)	$r_{\rm p/c/s}$ (pc)
1	Plummer	2.6×10^{-4}	1.5×10^{4}	-1.5×10^{38}	1.0×10^{-4}	0.013
1	CIS	3.2×10^{-4}	3.2×10^{4}	-7.2×10^{37}	6.0×10^{-5}	0.0032
1	NFW	3.2×10^{-4}	–	-7.8×10^{37}	6.7×10^{-5}	0.0014
2	Plummer	3.2×10^{-5}	7.0×10^{4}	-2.1×10^{37}	2.1×10^{-6}	0.0092
2	CIS	2.7×10^{-5}	1.2×10^{5}	-1.1×10^{37}	1.6×10^{-6}	0.0032
2	NFW	2.7×10^{-5}	–	-5.1×10^{37}	1.4×10^{-6}	0.011
3	Plummer	3.0×10^{-5}	8.1×10^{4}	-1.0×10^{37}	1.3×10^{-6}	0.0076
3	CIS	2.4×10^{-5}	2.0×10^{5}	-1.0×10^{37}	1.2×10^{-6}	0.0019
3	NFW	2.6×10^{-5}	–	-5.2×10^{37}	1.4×10^{-6}	0.0076

where $(\Delta E(b)/E)_{\rm fid}$ is the fractional energy input in an interaction with a fiducial star with mass $M_\star = 1\,{\rm M}_\odot$ and relative velocity $v = 300\,{\rm km\,s^{-1}}$.

3 APPLICATION TO MINI-HALOES

3.1 Density profiles

We use the following three benchmark density profiles.

(i) *Plummer sphere*

$$\rho(r) = \frac{\rho_0}{\left[1 + (r/r_{\rm p})^2\right]^{5/2}}. \tag{12}$$

This profile (Plummer 1915), which has a central core and asymptotes to r^{-5} at large radii, is commonly used to model star clusters. It is not a good fit to simulated CDM haloes or subhaloes; however, it is a convenient choice for testing the impulse approximation against numerical simulations as it has a simple form for the density and velocity distributions (see Aarseth, Hénon & Wielan 1974). In addition, the rapid fall-off of the density at large radii means that there are no subtleties involved in imposing a truncation radius (see e.g. Kazantzidis, Magorrian & Moore 2004), and the Plummer sphere is also stable when isolated.

(ii) *Cored isothermal sphere* (*CIS*)

$$\rho(r) = \rho_0 \frac{r^2 + 3r_{\rm c}^2}{\left(r^2 + r_{\rm c}^2\right)^2}. \tag{13}$$

The cored isothermal sphere is a better (although still not good) approximation to the mini-haloes, is amenable to analytic calculations and allows us to investigate the impact of a central core and more gradual fall-off at large radii to the fractional energy input.

(iii) *Navarro, Frenk & White* (*NFW*)

$$\rho(r) = \frac{\rho_0}{(r/r_{\rm s})[1 + (r/r_{\rm s})]^2}. \tag{14}$$

The NFW profile (Navarro, Frenk & White 1996, 1997) fits the density distribution, outside the very central regions, of simulated galactic scale and larger DM haloes well and is often used to model massive DM haloes. However, mini-haloes form monolithically, rather than by hierarchical mergers like 'standard' DM haloes, and it is not clear that they will have the same density profile. The NFW profile does, however, provide a reasonably good fit to the density profiles of the mini-haloes from Diemand et al.'s simulations.

We find the best fit for each of these profiles for the three typical haloes in fig. 2 of Diemand et al. (2005) using only the data points (density averaged within radial bins) at radii greater than the force resolution (using all the data points does not significantly change the best-fitting parameters). We refer to the haloes denoted by the squares, stars and circles in their figure as haloes 1, 2 and 3, respectively.

The CIS and NFW profiles have infinite mass and energy unless a cut-off radius is imposed by hand. For definiteness, and to allow comparison with previous work on mini-halo disruption, we use the radius at which the halo density is 200 times the cosmic mean density at $z = 26$ when Diemand et al.'s simulations are stopped and the sample haloes studied. For halo 1 $r_{200}(z = 26) = 0.03$ pc while for haloes 2 and 3 $r_{200}(z = 26) = 0.008$ pc. For the Plummer profile, a cut-off is not in principle needed; however, we use the same values for the radii for consistency.

In Table 1, we give the values of the Plummer, core and scale radii (as appropriate), the mass (M), initial energy per unit mass (E/M) and the structure parameters, $\alpha^2 R^2$ and β^2/R^2. Our values of the structure parameters are slightly different from those of Carr & Sakellariadou (1999) as they defined the cluster radii differently. Haloes 2 and 3 have roughly the same mass $\sim 10^{-6}\,{\rm M}_\odot$ depending at the tens of per cent level on the profile used. Halo 1 is a factor of $\sim$50 more massive.[2] We calculate the total energy by calculating the potential, and hence the velocity dispersion and kinetic and potential energy densities, from the density profiles. The truncation at finite radii means that the resulting haloes are not in virial equilibrium. For all three profiles for halo 1 and the CIS and NFW profiles for haloes 2 and 3, the deviation is relatively small. The best-fitting Plummer spheres for haloes 2 and 3 have $r_{\rm s} \sim \mathcal{O}(r_{200}(z = 26))$ and the resulting systems are far from virial equilibrium.

The values of α^2, which parametrizes the energy input for large impact parameter encounters, only vary by a factor of $\sim$2 between different haloes and density profiles reflecting the fact that the sample haloes have similar mean densities. However, β^2, which parametrizes the energy input in the $b \to 0$ limit varies significantly and is in fact infinite for the NFW profile. It can be seen from the definition of β^2, equation (6), that β^2 is formally infinite for any profile with a central cusp $\rho(r) \sim r^{-\gamma}$ with $\gamma \geqslant 1$. The WIMP

[2] It appears that $5.1 \times 10^{-6}\,{\rm M}_\odot$ for halo 1 in the caption of fig. 2 of Diemand et al. (2005) is a typo and should be $5.1 \times 10^{-5}\,{\rm M}_\odot$.

density cannot in fact become arbitrarily high in the central regions of a mini-halo; if the density becomes sufficiently high, the WIMPs will annihilate, reducing the density to some maximum value $\rho_{\rm max}$ so that the halo has a (small) core: $\rho(r) = \rho_{\rm max}$ for $r < r_{\rm core}$. The density and size of the core can be estimated by calculating the density for which the annihilation time-scale is less than the Hubble time (cf. Berezinsky, Gurevich & Zybin 1992):

$$\frac{\rho_{\rm max}\langle\sigma_{\chi\chi}v\rangle}{2m_\chi} < \frac{1}{10^{10}\ {\rm yr}}. \tag{15}$$

Using 'typical' values for the WIMP mass and velocity averaged cross-section, $m_\chi = 100\,{\rm GeV}$, $\langle\sigma_{\chi\chi}v\rangle = 3\times10^{-32}\,{\rm m^3\ s^{-1}}$, we find $\rho_{\rm max} = 4\times10^{-13}\,{\rm kg\,m^{-3}} = 4\times10^{13}\rho_{\rm c}(z=0)$. For the best-fitting NFW profiles, $r_{\rm core}\sim10^{-10}$ pc. Taking this effect into account leads to finite values for β^2, but they are still large ($\sim10^7$). The energy input only reaches its asymptotic value, however, for tiny ($\sim r_{\rm core}$), and hence extremely rare, impact parameters.

3.2 Simulations of star–mini-halo encounters

We use the DRAGON smooth particle hydrodynamics code (e.g. Goodwin, Whitworth & Ward-Thompson 2004a,b; Hubber, Goodwin & Whitworth 2006) with hydrodynamics turned-off as an *N*-body code. DRAGON uses a Barnes-Hut (1986)-type tree and we set the opening angle to be small to increase the accuracy of the force calculations between DM particles. The forces between DM particles and the star are all computed by direct summation. This physical situation, interaction of an extended body with a far more massive compact object, has, to our knowledge, not been studied numerically before and we carried out extensive testing to ensure the reliability of the results. In particular, the masses of the DM particles are a factor of $\sim\mathcal{O}(10^9)$ less massive than the perturbing star, requiring numerical care to be taken.

We generate the initial conditions for the Plummer sphere mini-haloes using the prescription of Aarseth et al. (1974), assuming that the haloes are initially in virial equilibrium. Left isolated, the mini-haloes remain in equilibrium, and the energy conservation of the code is $\sim10^{-5}$ over time-scales far in excess of a typical mini-halo–star interaction time-scale ($\sim$50 kyr). A star of mass $M_\star$ is then placed 1 pc away from the halo approaching it at velocity v, with an impact parameter b.

We conduct simulations with $N = 5000$ DM particles with a Plummer force softening between DM particles of $\epsilon = 10^{-3}$ pc. The forces due to the star are softened with a significantly smaller softening length of 10^{-4} pc. The softening between DM particles is rather large, but we wish to subdue any two-body interactions between DM particles. Tests conducted with $\epsilon = 10^{-4}$ and 10^{-2} pc show *no* difference in the results. Similarly, increasing the particle numbers to $N = 10\,000$ and 20 000, we found no significant (or systematic) changes. This convergence is not surprising as the energy input is entirely due to the encounter with the star whose force is accurately calculated with a low softening length, and we are only concerned with the energy input to the halo, and not in the details of relaxation and/or mass loss after the impulse has occurred (which will involve interactions between the halo particles and may require a larger number of particles for convergence e.g. Goerdt et al. 2006).

We ran a large ensemble of simulations covering a wide range of $M_\star$ –v–b parameter space: $0.215 < M_\star/{\rm M}_\odot < 30$, $1 < v/(1\,{\rm km\,s^{-1}}) < 400$[3] and $-5 < \log_{10}(b/1\,{\rm pc}) < 1$. With $N = 5000$, each simulation took an average of 20 min on a desktop PC.

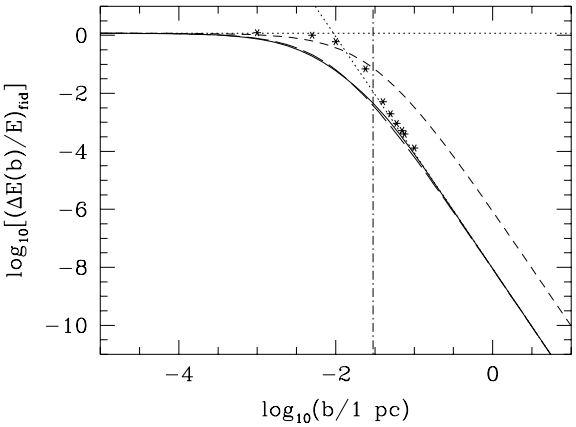

Figure 1. The fractional energy input, $(\Delta E(b)/E)_{\rm fid}$, in an interaction with a fiducial star with mass $M_\star = 1\,{\rm M}_\odot$ and relative speed $v = 300\,{\rm km\,s^{-1}}$ for the best-fitting Plummer profile for halo 1. The solid line from numerically integrating equation (8), the dotted lines asymptotic limits, equations (2) and (5), the short-dashed line using the original fitting function, equation (9), and the long-dashed line the modified fitting function, equation (10). The stars from numerical simulations. The dot–dashed line is the radius of the mini-halo.

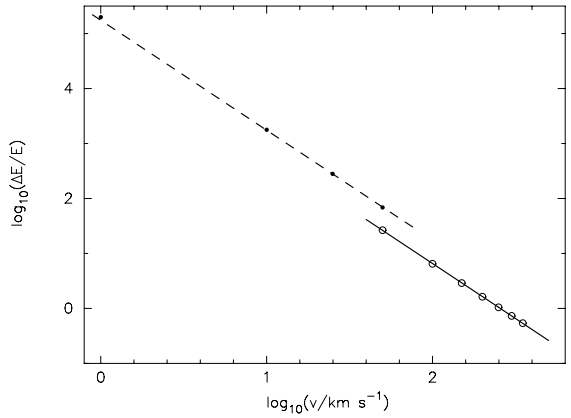

Figure 2. The fractional energy input, $\Delta E/E$, from simulations of the best-fitting Plummer profile for halo 1 as a function of relative velocity for encounters with a perturber of mass $M_\star = 1\,{\rm M}_\odot$. The open circles have an impact parameter of $b = 10^{-2}$ pc, while the filled circles have $b = 10^{-5}$ pc. The fractional energy input scales as v^{-2} as expected (lines of gradient -2 have been added to aid the eye).

3.3 Fractional energy input

The fractional energy input, $(\Delta E(b)/E)_{\rm fid}$, in an interaction with a fiducial star with mass $M_\star = 1\,{\rm M}_\odot$ and relative velocity $v = 300\,{\rm km\,s^{-1}}$ is plotted in Fig. 1 for the best-fitting Plummer sphere for halo 1. This fiducial velocity, chosen as an isothermal sphere with circular velocity $v_{\rm c} = 220\,{\rm km\,s^{-1}}$ [i.e. representing the Milky Way (MW)], has an rms speed of $270\,{\rm km\,s^{-1}}$. In reality, interactions will have a range of velocities and perturber masses. In Figs 2 and 3, we

[3] Although interactions with relative speeds at the lower end of this range are extremely rare, we consider them in order to test the validity of the impulse approximation.

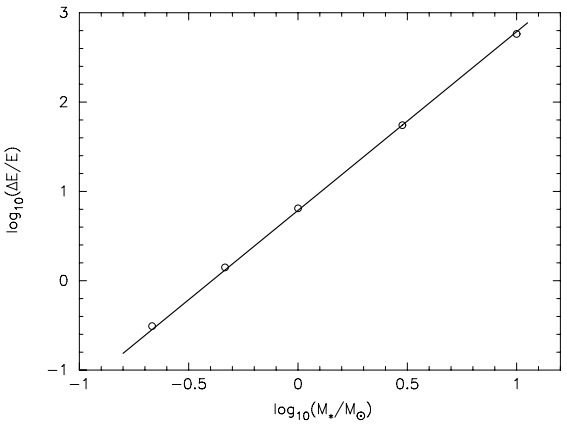

Figure 3. The fractional energy input, $\Delta E/E$, from simulations of the best-fitting Plummer profile for halo 1 as a function of perturber mass for encounters with a relative velocity $v = 100\,\mathrm{km\,s^{-1}}$ at an impact parameter of $b = 10^{-2}$ pc. The fractional energy input scales as $M_\star^2$ as expected (a line of gradient 2 has been added to aid the eye).

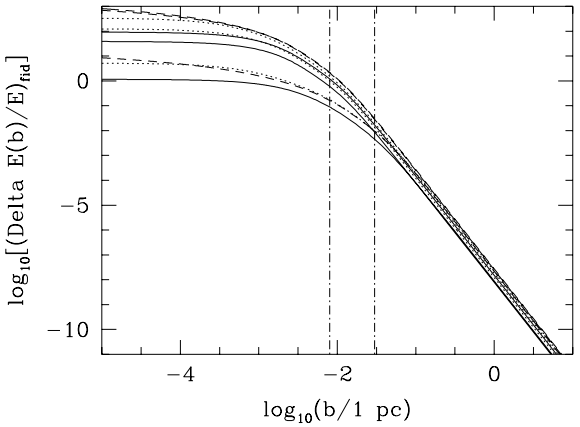

Figure 4. The fractional energy input in an interaction with a fiducial star with mass $M_\star = 1\,\mathrm{M}_\odot$ and relative speed $v = 300\,\mathrm{km\,s^{-1}}$, $(\Delta E(b)/E)_{\rm fid}$, calculated using equation (8) for the best-fitting Plummer (solid line), CIS (dotted line) and NFW (dashed line) profiles for (from bottom to top panel) haloes 1, 2 and 3. The dot–dashed lines are the radii of the mini-haloes (0.03 pc for halo 1, and 0.008 pc for haloes 2 and 3).

plot the fractional energy input as a function of relative velocity and perturber mass, showing that it scales as v^{-2} and $M_\star^2$, respectively, as expected from equation (2). In Fig. 2, we also show that the v^{-2} proportionality is independent of the impact parameter and holds down to very small [$\mathcal{O}(1\,\mathrm{km\,s^{-1}})$] relative velocities.

For a given perturber mass and relative velocity, we see from Fig. 1 that the large and small b asymptotic limits are in excellent agreement with the full analytic calculation using equation (8). As expected, the original fitting function significantly overestimates the energy input at large b. The modified fitting function, designed to reproduce the asymptotic limits, matches well the calculation using equation (8) for all b. In the simulations, however, the transition between the $b \ll R$ and $b \gg R$ regimes happens very rapidly and the energy input is well approximated, for all b, by the minimum of the asymptotic limits:

$$\Delta E(b) = \frac{G^2 M_\star^2 M}{v^2} \times \min\left(\frac{4\alpha^2 R^2}{3b^4}, \frac{3\beta^2}{R^2}\right). \tag{16}$$

In the $b \sim R$ regime, the energy input in the simulations is significantly larger than that from the analytic impulse approximation calculation. This may be indicating that in this regime, due to the asymmetry of the interaction, the $(\delta\boldsymbol{v}) \cdot \boldsymbol{v}$ term in the total energy input does not average to zero. It would be interesting to examine whether the energy input for $b \sim R$ depends on the mini-halo density profile.

In Fig. 4, we plot the fractional energy input from an interaction with a fiducial star with mass $M_\star = 1\,\mathrm{M}_\odot$ and relative speed $v = 300\,\mathrm{km\,s^{-1}}$ for the best-fitting profiles for all three haloes calculated using equation (8). The fractional energy input for close interactions, which is proportional to $\beta^2 M/ER$, varies by a factor of $\sim$3 for a given halo and is $\sim$100 times larger for the lighter haloes 2 and 3. This indicates that smaller, lighter mini-haloes are far more susceptible to disruption by close encounters. For large impact parameter interactions ($b \gg R$), the fractional energy input, which is proportional to $\alpha^2 MR^2/E$ varies only weakly (by a factor of $\sim$3) between haloes and profiles, with the spread in values for different profiles for a given halo being comparable to that for different haloes for a fixed profile.

This behaviour can be qualitatively understood by considering the asymptotic fractional energy input for a uniform density sphere (with $\rho = \rho_0$ for $r < R$ and $\rho = 0$ otherwise):

$$\frac{\Delta E(b)}{E} \propto \begin{cases} \frac{1}{\rho_0} & (b \gg R), \\ \frac{1}{\rho_0 R^4} & (b \ll R). \end{cases}$$

On galactic scales, the redshift at which a given scale goes non-linear, and hence the characteristic density of typical haloes, is strongly scale-dependent. The comoving scales corresponding to the mini-haloes [$k > \mathcal{O}(0.1\,\mathrm{pc^{-1}})$] entered the horizon during the radiation-dominated epoch, where CDM density perturbations grow only logarithmically. The size of the density perturbations, at a fixed redshift, on these scales is therefore only logarithmically dependent on the comoving wavenumber. Consequently, the redshift at which a given physical scale goes non-linear, and hence the characteristic density of the resulting haloes, is only weakly (roughly logarithmically) dependent on the scale (see e.g. Green et al. 2005). Neglecting this weak scale dependence and making the approximation that $\rho_0 \sim$ constant, $\Delta E/E \sim$ constant for $b \gg R$ and $\Delta E/E \sim M^{-4/3}$ for $b \ll R$. These scalings are in broad agreement with the trends found for the three sample haloes. The weak scale dependence of the redshift of non-linearity will lead to more-massive haloes typically having lower characteristic densities and hence being slightly more susceptible to disruption. This scale dependence is relatively small, however, and is comparable in magnitude to the dependence on the mini-halo density profile.

This behaviour, along with the results from the numerical simulations for the Plummer sphere, indicates that a reasonable approximation to the fractional energy input is given by a sudden transition between the asymptotic $b\langle\langle/\rangle\rangle R$ regimes:

$$\left(\frac{\Delta E}{E}\right)_{\rm fid} = \begin{cases} \left(\frac{\Delta E}{E}\right)_{\rm fid,s} \left(\frac{1\,\mathrm{pc}}{b}\right)^4 & b > b_{\rm s}, \\ \left(\frac{\Delta E}{E}\right)_{\rm fid,0} \left(\frac{1\,\mathrm{pc}}{b_{\rm s}}\right)^4 & b < b_{\rm s}, \end{cases}$$

where

$$\left(\frac{\Delta E}{E}\right)_{\rm fid,s} = \frac{4\alpha^2}{3} \frac{G^2\, M_\odot^2\, M R^2}{(300\,\mathrm{km\,s^{-1}})^2 (1\,\mathrm{pc})^4} \approx 1 \times 10^{-8} \tag{17}$$

is the asymptotic large-b slope, and the transition between the two regimes occurs, for the three sample haloes, at

$$b_{\rm s} = \left(\frac{4\alpha^2}{9\beta^2}\right)^{1/4} R = A^{1/4} R \approx (0.3\text{–}0.45) R. \quad (18)$$

The large variation in the value of β^2 for the different haloes/profiles has a relatively small (less than a factor of 2) effect on the value of A; however, taking this R–M dependence into account is crucial for obtaining the correct $b \ll R$ asymptotic behaviour. The NFW profile, however, is slightly problematic. As discussed above, its (very large) asymptotic value of β^2 is only reached for tiny impact parameters. A reasonable prescription for this profile is to use the asymptotic fractional energy input at $b = 0.1R$ to calculate the value of β^2.

It should be emphasized that the representative sample haloes studied in detail by Diemand et al. presumably form from 'typical', $\sim$1–2σ, fluctuations. Similarly, our discussion (above) of the scaling of the energy input with the halo mass implicitly assumed that the haloes form from similar-sized overdensities. Mini-haloes which form from rarer large overdensities will be denser and hence more resilient to disruption (Berezinsky et al. 2003, 2006; Green et al. 2004, 2005). More specifically, in the spherical collapse model, a halo forming on a given comoving scale from an $N\sigma$ fluctuation will have $R \propto 1/N$, $M \sim$ constant, and characteristic density $\rho \propto N^3$ (Green et al. 2005). We therefore expect that the fractional energy input in close encounters will be far smaller for haloes formed from rarer, larger, fluctuations. The quantitative effect on the fractional energy input will depend on exactly how the characteristic density and density profile scale with the size of the overdensity from which the mini-halo forms.

3.4 One-off disruption

We now use the criterion $\Delta E(b_{\rm c})/E = 1$ and the sudden transition approximation developed in Section 3.3 above, to estimate the critical impact parameter $b_{\rm c}$, below which the energy input in a single encounter is larger than the binding energy. Taken at face value, an energy input $\Delta E(b)/E > 1$ might appear to imply that the mini-halo is completely disrupted. In reality, however, the reaction of a system to a sudden change in energy, and in particular the relationship between the energy input and the mass lost, is non-trivial (see e.g. Aguilar & White 1985; Goodwin 1997; Gnedin & Ostriker 1999; and, for the specific case of mini-halo interactions with stars, Goerdt et al. 2006). The system will expand and attempt to revirialize, and during this process two-body encounters will redistribute energy between particles. The simple criterion $\Delta E(b_{\rm c})/E = 1$ allows us to make an estimate of the impact parameter below which a mini-halo will lose a substantial fraction of its mass in a single encounter (which for compactness we refer to as 'one-off disruption'). A detailed calculation of the mass loss, however, requires numerical simulations of the revirialization and energy redistribution processes (cf. Goerdt et al. 2006).

One-off disruption cannot occur if the asymptotic fractional energy input as b tends to zero is less than 1. This is the case if

$$\left(\frac{M_\star}{\rm M_\odot}\frac{300\,{\rm km\,s^{-1}}}{v}\right) < \left(\frac{\Delta E}{E}\right)^{-1/2}_{\rm fid,s}\left(\frac{b_{\rm s}}{1\,{\rm pc}}\right)^2. \quad (19)$$

Otherwise,

$$\frac{b_{\rm c}}{1\,{\rm pc}} = \left(\frac{\Delta E}{E}\right)^{1/4}_{\rm fid,s}\left(\frac{M_\star}{\rm M_\odot}\frac{300\,{\rm km\,s^{-1}}}{v}\right)^{1/2}. \quad (20)$$

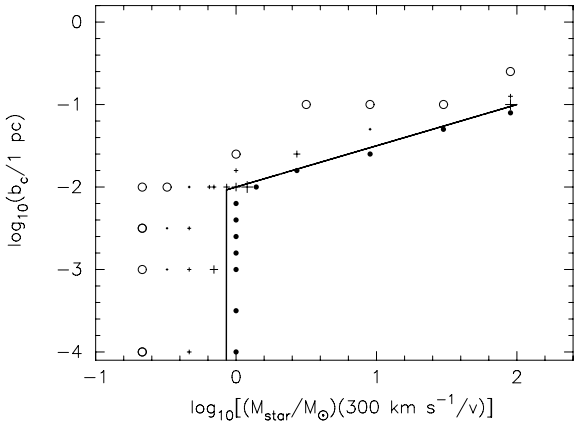

Figure 5. The maximum impact parameter for which one-off disruption can occur, $b_{\rm c}$, for the best-fitting Plummer profile for halo 1 (which has $R = 0.03$ pc and $r_{\rm p} = 0.013$ pc). The solid line shows the analytic calculation using the sudden transition approximation, equation (20). The symbols are the results of numerical simulations: the open circles for $(\Delta E(b)/E) < 0.05$, the filled circles for $(\Delta E(b)/E) > 1$ (potential one-off disruption) and the size of crosses is proportional to $(\Delta E(b)/E)$ in the intermediate regime.

In Fig. 5, we plot $b_{\rm c}$ as a function of $M_\star/v$ for the best-fitting Plummer profile for halo 1 calculated using the analytic expressions derived from the sudden transition approximation (equations 19 and 20). We also plot the energy input in numerical simulations, demonstrating that the sudden transition approximation provides a good fit to the transition between the $[\Delta E(b)/E] > 1$ and $[\Delta E(b)/E] < 1$ regimes. The critical impact parameter is quite sensitive to the properties of the perturbing star. Thus, a full calculation of mini-halo disruption will have to take into account the stellar mass and velocity distributions.

4 IMPLICATIONS AND OPEN ISSUES

4.1 Disruption time-scales

As discussed in the Introduction section (see also Zhao et al. 2007; Angus & Zhao 2006; Goerdt et al. 2006), an accurate calculation of the mini-halo survival probability distribution will require the combination of simulations of mass loss with orbits in a realistic Galactic potential. In this section though, we use the results of our energy input studies in Section 3, in particular the sudden transition approximation, to estimate the disruption time-scales for typical mini-haloes as a function of mass for some benchmark orbits.

4.1.1 One-off disruption

For the simplified situation where all perturbers have the same velocity and mass, the rate at which encounters with impact parameter smaller than $b_{\rm c}$, the critical value for which the energy input is larger than the binding energy, occur is

$$\frac{{\rm d}N}{{\rm d}t} = \pi n v b_{\rm c}^2, \quad (21)$$

where n is the perturber number density. Taking the stellar mass and relative speed to be fixed at $M_\star = 0.5\,{\rm M_\odot}$ and $v = 270\,{\rm km\,s^{-1}}$, respectively, halo 1 will never undergo one-off disruption, while for haloes 2 and 3, using the sudden transition approximation, the critical impact parameter for one-off disruption is 0.0075 pc. Taking

a disc mass density of $0.023\,\mathrm{M}_\odot\,\mathrm{pc}^{-3}$,[4] we find a one-off disruption time-scale, $t_{\rm dis} \approx 1/(\mathrm{d}N/\mathrm{d}t)$, for haloes 2 and 3 of 0.5 Gyr for (rare) halo orbits which lie entirely within the Galactic disc for $b_{\rm c} = 0.0075$ pc. This indicates that a 10^{-6}-$\mathrm{M}_\odot$ mini-halo which spends most of its time in the disc will undergo a change in its energy which is large compared to its binding energy and hence lose a significant fraction of its mass. The density of stars in the spheroid is significantly smaller, $\sim 10^{-5}\,\mathrm{M}_\odot\,\mathrm{pc}^{-3}$, and declines rapidly with increasing Galactocentric radius; therefore, mini-haloes on orbits which never pass through the disc are extremely unlikely to experience a close encounter which removes most of their mass. Most mini-haloes will, however, be on intermediate orbits and spend some fraction of their time passing through the disc. For instance, a mini-halo on a circular polar orbit at the solar radius with speed $v = 270\,\mathrm{km\,s}^{-1}$ would spend a fraction $\sim$0.08 of its time within the disc, giving a disruption time-scale of 6 Gyr. Therefore, in the inner regions of the MW where orbits pass through the disc, the time-scale on which $10^{-6}\,\mathrm{M}_\odot$ haloes which experience significant mass loss in a single interaction is of order the age of the MW and a more sophisticated calculation is required.

Generalizing to the more realistic case of a population of perturbers with a range of speeds and masses, the rate at which interactions with impact parameters smaller than the critical impact parameter for potential one-off disruption to occur becomes

$$\frac{\mathrm{d}N}{\mathrm{d}t} = \int\int \frac{\mathrm{d}^2 n}{\mathrm{d}M_\star \mathrm{d}v} \pi v b_{\rm c}^2 \left(\frac{M_\star}{v}\right) \mathrm{d}M_\star \mathrm{d}v, \tag{22}$$

where $\mathrm{d}^2 n/\mathrm{d}M_\star\,\mathrm{d}v$ is the number density of stars with mass between $M_\star$ and $M_\star + \mathrm{d}\,M_\star$ and relative speed between v and $v + \mathrm{d}v$. We assume that mass and speed distributions are independent so that

$$\frac{\mathrm{d}^2 n}{\mathrm{d}M_\star \mathrm{d}v} = \frac{\mathrm{d}n_1}{\mathrm{d}M_\star}\frac{\mathrm{d}n_2}{\mathrm{d}v}. \tag{23}$$

For the mass distribution, we use the Kroupa (2002) stellar mass function (MF)

$$\frac{\mathrm{d}n_1}{\mathrm{d}M_\star} \propto \begin{cases} M_\star^{-1.3} & 0.08 < M_\star/\mathrm{M}_\odot < 0.5, \\ M_\star^{-2.3} & 0.5 < M_\star/\mathrm{M}_\odot < 50, \end{cases}$$

which is a good fit to the local field population (see also Chabrier 2001). We ignore the contribution from brown dwarfs as, due to the $M_\star^2$ factor, this population – whilst numerous – makes only a small contribution to the disruption rate. We normalize the MF so that the total mass density is $0.023\,\mathrm{M}_\odot\,\mathrm{pc}^{-3}$. We take the speed distribution to be Gaussian about the mini-halo speed, $V = 270\,\mathrm{km\,s}^{-1}$:

$$\frac{\mathrm{d}n_2}{\mathrm{d}v} = \frac{1}{(2\pi)^{1/2}\sigma_\star} \exp\left[-\frac{(v-V)^2}{2\sigma_\star^2}\right], \tag{24}$$

with stellar speed dispersion $\sigma_\star = 25\,\mathrm{km\,s}^{-1}$.

The resulting one-off disruption time-scales are 0.8 Gyr for halo 1 and 0.5 Gyr for haloes 2and 3. For haloes 2 and 3, the disruption time is similar to that calculated assuming delta-function mass and speed distributions. The main result though is that, once the spread in stellar masses is taken into account, the more-massive halo 1 can undergo one-off disruption on a time-scale smaller than the age of the MW. Taking into account the spread of masses and velocities is therefore crucial for calculating the mass threshold above which mini-haloes will not lose a significant fraction of their mass in a single encounter.

[4] This corresponds to a surface density of $46\,\mathrm{M}_\odot\,\mathrm{pc}^{-2}$ (Kuijken & Gilmore 1989) over a height of 2 kpc.

4.1.2 *Disruption through multiple encounters*

The time-scale on which a mini-halo will lose a significant fraction of its mass as a result of the cumulative effects of encounters with $\Delta E(b)/E < 1$ (which, for compactness, we refer to a 'disruption through multiple encounters') can be estimated as

$$t_{\rm dis} = \frac{E}{(\mathrm{d}E/\mathrm{d}t)_{\rm tot}}. \tag{25}$$

This is likely to be an overestimate; the mini-halo density profile changes in response to interactions and this appears to reduce the effect of cumulative interactions (Goerdt et al. 2006).

Starting, once again, with the simplifying assumption that all stars have the same mass and relative velocity,

$$\frac{(\mathrm{d}E/\mathrm{d}t)_{\rm tot}}{E} = 2\pi \int_{b_{\rm c}}^{\infty} n v \frac{\Delta E(b)}{E} b\,\mathrm{d}b, \tag{26}$$

and taking the same parameter values as above we find, for orbits which lie entirely within the disc, $t_{\rm dis} = 0.4$ Gyr for halo 1 and $t_{\rm dis} = 0.5$ Gyr for haloes 2 and 3. The shorter time-scale for multiple disruption for halo 1 reflects the fact that it cannot undergo one-off disruption and hence $b_{\rm c} = 0$, whereas for haloes 2 and 3 $b_{\rm c} = 0.0075$ pc.

Generalizing to a distribution of masses and relative velocities, the fractional energy input rate becomes

$$\frac{(\mathrm{d}E/\mathrm{d}t)_{\rm tot}}{E} = 2\pi \int\int \left[\int_{b_{\rm c}(M_\star/v)}^{\infty} \frac{\mathrm{d}^2 n}{\mathrm{d}M_\star \mathrm{d}v} v b \frac{\Delta E(b)}{E} \mathrm{d}b\right] \mathrm{d}v\,\mathrm{d}M_\star. \tag{27}$$

We now find $t_{\rm dis} = 0.6$ Gyr for halo 1 and $t_{\rm dis} = 0.5$ Gyr for haloes 2 and 3.

The net energy input rate is the sum of the energy input rates from 'one-off' and 'multiple disruption', and the net disruption time-scale will be shorter than the characteristic time-scales for 'one-off' and 'multiple disruption' individually.

We have assumed that the stellar density within the disc is uniform. In general, clustering will increase the spread in disruption time-scales for mini-haloes of a given mass. In addition, most stars (certainly those with $M_\star > 0.5\,\mathrm{M}_\odot$) are in fact in binary systems (e.g. Goodwin et al. 2006) and will cause a greater disruptive effect than a single star. Systems whose separations are significantly less than the mini-halo radius (<1000 au) will effectively combine the primary and secondary masses and, due to the $M_\star^2$ dependence of the energy input, even fairly low-mass secondaries may play an important role. We estimate that $\sim$30–40 per cent of stars with $M_\star > 1\,\mathrm{M}_\odot$ may have a large enough companion to increase the energy input by a factor >2.[5] Even very low mass stars ($<0.5\,\mathrm{M}_\odot$) have a binary frequency of $\sim$30 per cent (Fischer & Marcy 1992), and so the fraction of M dwarfs with a companion that could very significantly increase the energy input is $\sim$15–20 per cent. Thus, an accurate calculation of mini-halo disruption will have to combine simulations of mini-halo orbits in a realistic potential with an accurate model of the stellar distribution, including the binary fraction, within the disc.

[5] A companion with a mass ratio greater than 0.4 will increase the energy input by more than $(1.4)^2 \sim 2$, and we assume a binary fraction of $\sim$60 per cent (see Duquennoy & Mayor 1991).

4.2 Mass dependence

We have seen that more-massive mini-haloes are less susceptible to disruption. It is therefore interesting to investigate the mass dependence of the disruption time-scales. Furthermore, the WIMP damping scale, and hence the mass of the smallest mini-haloes, depends on the properties (elastic scattering cross-section and mass) of the WIMPs. For generic WIMPs, Green et al. (2005) found a spread in the minimum mass of several orders of magnitude, while Profumo, Sigurdson & Kamionkowski (2006) have recently found that in the Minimal Supersymmetric Standard Model the minimum mass may vary between 10^{-12} and $10^{-4}\,\mathrm{M}_{\odot}$.

The correct mass dependence of the small-b energy input, and hence the transition radius, $b_{\rm s}$, is not known. We consider two scalings which should give an indication of the trend, and also the uncertainties. First, motivated by the qualitative understanding of the mass dependence of the asymptotic limits of the fractional energy input found in Section 3.3, we once more consider a uniform density sphere. For uniform density spheres (with constant density), the profile parameter $A(=4\alpha^2/9\beta^2)$ is independent of the radius/mass and hence $b_{\rm s} \propto R \propto M^{1/3}$. For the three sample haloes, A decreases slightly with increasing mass (albeit with significant scatter between profiles and between haloes 2 and 3), and $b_{\rm s} \propto M^{0.2}$. We use both these scalings, normalizing in both cases to $b_{\rm s} = 0.004\,\mathrm{pc}$ at $M = 10^{-6}\,\mathrm{M}_{\odot}$. The correct variation might be significantly different from either of these scalings, however, and needs to be determined from the profiles of simulated haloes with a range of masses. In Fig. 6, we plot the resulting disruption times for an orbit entirely within the disc (for other orbits the disruption time-scales scale roughly as the fraction of time spent within the disc) as a function of mini-halo mass, using the sudden transition approximation with $(\Delta E/E)_{\rm fid,s} = 10^{-8}$.

For very small mini-haloes, $M < 10^{-7}\,\mathrm{M}_{\odot}$, the one-off and multiple-encounter disruption time-scales are independent of mass, and are roughly equal. The mass independence is because for these small mini-haloes the transition impact parameter is smaller than the critical impact parameter for the range of $M_{\star}$ and v values considered, $b_{\rm s} < b_{\rm c}(M_{\star}/v)$, so that $b_{\rm c}(M_{\star}/v)$ lies in the $\Delta E(b)/E \propto b^{-4}$ regime and is independent of the mini-halo mass. The approximate equality of the one-off and multiple disruption time-scales can be understood by considering the simplified case of a delta-function mass/velocity distribution once more. Using the sudden-transition approximation, both disruption time-scales are then equal to $[\pi n v\,(M_{\star}/\mathrm{M}_{\odot})(300\,\mathrm{km\,s^{-1}}/v)\,(\Delta E/E)^{1/2}_{\rm fid,s}(1\,\mathrm{pc})^2]^{-1}$ if $b_{\rm s} < b_{\rm c}$.The more rapid scaling of $b_{\rm s}$, with M ($M^{0.33}$ versus $M^{0.2}$) also leads to larger values of $t_{\rm dis}$. The size of these differences increases with increasing mini-halo mass. The exact disruption time-scales of more-massive mini-haloes will depend on the mass dependence of the impact parameter at which the transition between close and distant encounters occurs and also how rapidly this transition occurs.

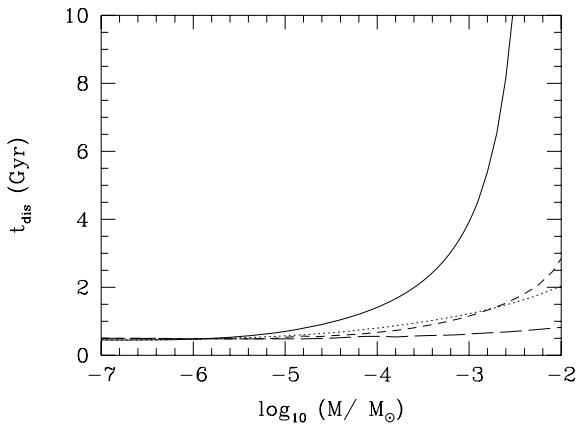

Figure 6. The disruption time-scales for an orbit entirely within the disc as a function of mini-halo mass. The solid line: one-off disruption assuming $b_{\rm s} \propto M^{0.33}$, the dotted line: one-off disruption assuming $b_{\rm s} \propto M^{0.2}$, the short-dashed line: multiple disruption assuming $b_{\rm s} \propto M^{0.33}$, and the long-dashed line: multiple disruption assuming $b_{\rm s} \propto M^{0.2}$.

4.3 Mini-halo radius

In common with other studies (Moore et al. 2005; Zhao et al. 2005, 2007), we have taken the mini-halo radii to be the radius at which the density is 200 times the critical density at $z = 26$ [the redshift at which Diemand et al. (2005) stopped their simulations and plotted the profiles of their sample haloes], $r_{200}(z = 26)$. The densities of simulated haloes do not decline sharply to zero beyond a given radius, however, and, if the mini-haloes remained isolated beyond this redshift their nominal radii (and hence masses and binding energies) would increase as the background density decreases. As an extreme example, if halo 1 remained isolated to $z = 0$ then, assuming a NFW density profile, its present-day radius would be $\sim$0.7 pc, its mass would a factor of $\sim$3 larger and, using equations (2) and (5), the fractional energy input in small (large) b encounters would be substantially decreased (increased). The value used for the mini-halo radius therefore has a potentially significant effect on calculations of the fractional energy input.

Once a mini-halo is accreted on to a larger halo, it no longer accretes further mass on to itself and it is also subject to the tidal field of the parent halo. For a mini-halo orbiting within a MW-like parent halo, the tidal radius is only comparable to $r_{200}(z = 26)$ for very small, of the order of a few kpc, Galactocentric radii. The radius of a mini-halo which does not pass through the very central regions of the MW will be the smaller of the tidal radius and the radius at the time of accretion [both of which are larger than $r_{200}(z = 26)$]. The redshift at which accretion occurs will, however, be different for different mini-haloes with the same initial properties. A detailed calculation of mini-halo evolution will therefore have to include the mini-halo merger histories. The majority of mini-haloes, in particular those which pass close to the solar radius and are hence most relevant for WIMP direct and indirect searches, will be accreted on to larger haloes not long after $z = 26$ and hence $r_{200}(z = 26)$ should be a reasonable estimate of their radii.

5 DISCUSSION

We have studied the energy input into earth-mass mini-haloes in interactions with stars. Using the impulse approximation (see Spitzer 1958; Gerhard & Fall 1983; Carr & Sakellariadou 1999), we have calculated the energy input as a function of impact parameter for a range of mini-halo density profiles. We also used the DRAGON code (e.g. Goodwin et al. 2004a,b; Hubber et al. 2006) to simulate interactions with Plummer sphere haloes. We found excellent agreement with the impulse approximation in the asymptotic limits $b \ll R$ (where b is the impact parameter and R is the mini-halo radius) with a rapid transition at $b \sim 0.1\,R$ between these regimes. We also verified the scaling of the fractional energy input with stellar mass and relative velocity.

Using analytic calculations, we find that the fractional energy input for large impact parameters, $b \gg R$, appears to be fairly independent of the mini-halo mass, varying by a factor of $\sim$2 for haloes with masses which differ by a factor of $\sim$50 with a similar variation for different density profiles. This behaviour probably reflects the fact that the haloes form at roughly the same time and hence have similar characteristic densities. The fractional energy input in the $b \rightarrow 0$ limit depends quite strongly on the mini-halo mass (being larger for lighter haloes) and is also dependent on the central density profile. For the NFW profile, which has asymptotic inner density profile $\rho \propto r^{-1}$, the fractional energy input only becomes significantly larger than that for the cored density profiles at tiny, and hence extremely rare, impact parameters, that is, $b \ll 10^{-3}R$. This divergence is therefore essentially unimportant for our calculations; however, the central regions of haloes with cuspy density profiles may be able to survive even after substantial energy input/mass loss (e.g. Moore et al. 2005; Goerdt et al. 2006). Motivated by the results of our analytic and numerical calculations, we formulate a fitting function for the fractional energy input as a function of impact parameter, which we refer to as the 'sudden transition' approximation. The slope of the fractional energy input at large impact parameters is constant, while the impact parameter which characterizes the transition between the limits is mini-halo mass-dependent.

We also investigated the dependence of the critical impact parameter, b_c, for which the energy input is larger than the mini-halo binding energy on the mini-halo mass and also the relative speed and mass of the interacting star. As expected from the fractional energy input calculations, for slow encounters with massive stars, b_c is independent of the mini-halo mass. There is a critical value of $(M_\star/v)$, which increases with increasing halo mass, below which the energy input is always smaller than the binding energy. For all values of $(M_\star/\,\mathrm{M}_\odot)(300\,\mathrm{km\,s^{-1}}/v)$, the results of our Plummer sphere simulations are in good agreement with the analytic expressions for b_c from the sudden transition approximation.

We then use the sudden transition approximation to estimate the time-scales for one-off and multiple disruption for mini-haloes in the MW as a function of mini-halo mass, using the approximate destruction criterion $\Delta E/E = 1$. We take into account the stellar and velocity distribution and note that binary stars can cause a significantly greater energy input than single stars, due to their greater effective mass. For light mini-haloes with $M < \mathcal{O}(10^{-7}\,\mathrm{M}_\odot)$, the disruption time-scales are independent of mini-halo mass and, for a mini-halo in the inner regions of the MW on a typical orbit which spends a few per cent of its time passing through the disc, are comparable to the age of the MW. For more-massive mini-haloes, $M > \mathcal{O}(10^{-4}\,\mathrm{M}_\odot)$, the disruption time-scale estimates increase rapidly with increasing mass, suggesting that the majority of these mini-haloes will not be disrupted by stellar encounters. It is important to caution, however, that the relationship between the energy input and the change in the bound mass is not straightforward. In particular, the mini-halo density profile evolves so that successive multiple encounters are less effective than would naively be expected and even if the energy input in a single encounter is much larger than the binding energy a small fraction of the mass can remain bound (Goerdt et al. 2006). Therefore, these simple estimates are likely to be overestimates of the actual disruption time-scales.

Finally, we discussed the dependence of the fractional energy input on the mini-halo radius assumed. To be consistent with other studies (Moore et al. 2005; Zhao et al. 2005, 2007), we took the radius to be the radius at which the density is 200 times the critical density at $z = 26$, the redshift at which Diemand et al. (2005) stopped their simulations and plotted the profiles of their sample haloes. This is a somewhat arbitrary definition, however; the densities of simulated haloes do not decline to zero beyond this radius and as the background density decreases the nominal radius increases. The physical extent/radius will in fact be that at the time of accretion on to a larger halo, or the tidal radius if this is smaller. The tidal radius within a MW-like parent halo is only smaller than $r_{200}(z = 26)$, at small Galactocentric radii, however, the majority of mini-haloes will be accreted on to larger haloes shortly after this redshift, so in practice $r_{200}(z = 26)$ should be a reasonable estimate of the radius of most mini-haloes.

A complete calculation of the disruption of mini-haloes will need to take into account their merger histories, simultaneously and consistently incorporate disruption due to encounters with stars and tidal stripping. Mini-haloes formed from rare, large-density fluctuations, will be denser, and hence more resilient to disruption, than typical mini-haloes and this will also need to be included.

ACKNOWLEDGMENTS

AMG is supported by the PPARC and SPG by the UK Astrophysical Fluids Facility (UKAFF). We are grateful to Tobias Goerdt and Simon White for useful comments/discussion.

REFERENCES

Aarseth S., Hénon M., Wielan R., 1974, A&A, 37, 183
Aguilar L. A., White S. D. M., 1985, ApJ, 295, 374
Angus G. W., Zhao H., 2006, preprint (astro-ph/0608580)
Barnes J., Hut P., 1986, Nat, 324, 446
Berezinsky V., Gurevich A. V., Zybin K. P., 1992, Phys. Lett. B, 294, 221
Berezinsky V., Dokuchaev V., Eroshenko Y., 2003, Phys. Rev. D, 68, 103003
Berezinsky V., Dokuchaev V., Eroshenko Y., 2006, Phys. Rev. D, 73, 063504
Bertone G., Hooper D., Silk J., 2005, Phys. Rep., 405, 279
Carr B. J., Sakellariadou M., 1999, ApJ, 516, 195
Chabrier G., 2001, ApJ, 554, 1274
Diemand J., Moore B., Stadel J., 2005, Nat, 433, 389
Duquennoy A., Mayor M., 1991, A&A, 248, 485
Fischer D. A., Marcy G. W., 1992, ApJ, 396, 178
Gerhard O. E., Fall S. M., 1983, MNRAS, 203, 1253
Gnedin O. Y., Ostriker J. P., 1999, ApJ, 513, 626
Goerdt T., Gnedin O. Y., Moore B., Diemand J., Stadel J., 2006, preprint (astro-ph/0608495)
Goodwin S. P., 1997, MNRAS, 284, 785
Goodwin S. P., Whitworth A. P., Ward-Thompson D., 2004a, A&A, 414, 633
Goodwin S. P., Whitworth A. P., Ward-Thompson D., 2004b, A&A, 423, 169
Goodwin S. P., Kroupa P., Goodman A., Burkert A., 2006, 'Protostars and Planets V'. Preprint (astro-ph/0603233)
Green A. M., Hofmann S., Schwarz D. J., 2004, MNRAS, 353, L23
Green A. M., Hofmann S., Schwarz D. J., 2005, JCAP, 08, 003
Hofmann S., Schwarz D. J., Stöcker H., 2001, Phys. Rev. D, 64, 083507
Hubber D. A., Goodwin S. P., Whitworth A. P., 2006, A&A, 450, 881
Kazantzidis S., Magorrian J., Moore B., 2004, ApJ, 601, 37
Klypin A., Kravtsov A. V., Valenzuela O., Prada F., 1999, ApJ, 522, 82
Kroupa P., 2002, Sci, 295, 82
Kuijken K., Gilmore G., 1989, MNRAS, 289, 605
Loeb A., Zaldarriaga M., 2005, Phys. Rev. D, 71, 103520
Moore B., 1993, ApJ, 413, L93
Moore B., Ghigna S., Governato F., Lake G., Quinn T., Stadel J., Tozzi P., 1999, ApJ, 524, L19

Moore B., Diemand J., Stadel J., Quinn T., 2005, preprint (astro-ph/0502213)
Navarro J. F., Frenk C. S., White S. D. M., 1996, ApJ, 462, 563
Navarro J. F., Frenk C. S., White S. D. M., 1997, ApJ, 490, 493
Oguri M., Lee J., 2004, MNRAS, 355 120
Peñarrubia J., Benson A. J., 2005, MNRAS, 364, 977
Plummer H. C., 1915, MNRAS, 76, 107
Profumo S., Sigurdson K., Kamionkowski M., 2006, Phys. Rev. Lett., 97 031301
Spitzer L. Jr., 1958, ApJ, 127, 17
Schwarz D. J., Hofmann S., Stöcker H., 2001, in Horvath D., Levai P., Patkos A., eds, Proc. High Energy Phys. Online only ref: astro-ph/0110601
Taylor J. E., Babul A., 2004, MNRAS, 348, 811
Zenter A., Bullock J., 2003, MNRAS, 348, 811
Zhao H., Taylor J. E., Silk J., Hooper D., 2005, preprint (astro-ph/0502049)
Zhao H., Hooper D., Angus G. W., Taylor J. E., Silk J., 2007, ApJ, 654, 697

This paper has been typeset from a TEX/LATEX file prepared by the author.